RESEARCH ARTICLE

Macromolecular Rapid Communications
www.mrc-journal.de

Engineering Sulfur-Containing Polymeric Fire-Retardant Coatings for Fire-Safe Rigid Polyurethane Foam

Yang Fang, Zhewen Ma, Dewang Wei, Youming Yu, Lei Liu,* Yongqian Shi, Jiefeng Gao, Long-Cheng Tang, Guobo Huang,* and Pingan Song**

With the advantages of lightweight and low thermal conductivity properties, polymeric foams are widely employed as thermal insulation materials for energy-saving buildings but suffer from inherent flammability. Flame-retardant coatings hold great promise for improving the fire safety of these foams without deteriorating the mechanical-physical properties of the foam. In this work, four kinds of sulfur-based flame-retardant copolymers are synthesized via a facile radical copolymerization. The sulfur-containing monomers serve as flame-retardant agents including vinyl sulfonic acid sodium (SPS), ethylene sulfonic acid sodium (VS), and sodium p-styrene sulfonate (VSS). Additionally, 2-hydroxyethyl acrylate (HEA) and 4-hydroxybutyl acrylate are employed to enable a strong interface adhesion with polymeric foams through interfacial H-bonding. By using as-synthesized waterborne flame-retardant polymeric coating with a thickness of 600 µm, the coated polyurethane foam (PUF) can achieve a desired V-0 rating during the vertical burning test with a high limiting oxygen index (LOI) of >31.5 vol%. By comparing these sulfur-containing polymeric fire-retardant coatings, poly(VS-*co*-HEA) coated PUF demonstrates the best interface adhesion capability and flame-retardant performance, with the lowest peak heat release rate of 166 kW m^{-2} and the highest LOI of 36.4 vol%. This work provides new avenues for the design and performance optimization of advanced fire-retardant polymeric coatings.

1. Introduction

Rigid polyurethane foam (PUF) represents one of the most important building thermal insulation materials; because of its good compressive strength, low density, and low thermal conductivity properties.[1–3] However, because of its organic composition and highly cellular structure, PUF suffers from intrinsic flammability with a low limiting oxygen index (LOI) of ≈19.5 vol%.[4] Brominated compounds as industrial flame retardants (FRs) can effectively enhance the flame retardancy of PUF.[5,6] Unfortunately, regulations have restricted the use of some halogenated FRs with the increasing awareness of environmental concerns and sustainable development.[7–9] As a result, it is imperative to develop halogen-free flame-retardant PUF without significantly compromising its mechanical-physical properties.[10,11]

The halogen-free FRs used for PUF are generally divided into i) reactive, ii) additive, and iii) coating types, which mainly consist of phosphorus, nitrogen, silicon, or sulfur elements.[12,13] Reactive FRs (e.g., tetrabromobisphenol A [TBBPA]

Y. Fang, D. Wei, Y. Yu
College of Chemistry and Materials Engineering
Zhejiang A&F University
Hangzhou 311300, China
E-mail: yuyouming@zafu.edu.cn

Z. Ma
Interdisciplinary Materials Research Center
College of Materials Science and Engineering
Tongji University
Shanghai 201804, P. R. China

L. Liu
College of Environment and Safety Engineering
Qingdao University of Science and Technology
Qingdao 266045, China
E-mail: leiliu@qust.edu.cn

L. Liu
Centre for Further Materials
University of Southern Queensland
Springfield Central, QLD 4300, Australia

Y. Shi
College of Environment and Safety Engineering
Fuzhou University
2 Xueyuan Road, Fuzhou 350116, China

J. Gao
School of Chemistry and Chemical Engineering
Yangzhou University
Yangzhou 225002, China

The ORCID identification number(s) for the author(s) of this article can be found under https://doi.org/10.1002/marc.202400068

DOI: 10.1002/marc.202400068

and tetrabromophthalic anhydride [TBPA]) can serve as polyols to participate in the curing process of RPUF,[14] but their unsatisfied flame-retardant efficiency significantly limits their practical applications.[15] The additive FRs feature higher flame retardancy and higher structural diversity than the reactive ones, such as ammonium polyphosphate (APP) and expandable graphite (EG).[16–18] But their poor interfacial compatibility often leads to degraded mechanical properties as they cannot participate in the foaming process.[19,20]

Compared to additive FRs, flame-retardant coatings demonstrate overwhelming advantages because they maintain the bulk properties of PUF.[21,22] Recently, many efforts have been reported to create fire-resistant coatings for PUF. For instance, Chen et al.[23] treated PUF with alginate/clay aerogel via the freeze-drying method. Compared to the untreated PUF, the resultant foam showed a high LOI of 60 vol% with a 32% reduction in the peak heat release rate (PHRR). However, the aerogel in the porous foam deteriorated the thermal conductivity. Huang et al.[24] fabricated flame-retardant PUF by employing a UV-curable intumescent coating. The treated PUF exhibited an LOI value of 24.8 vol% and a 33.2% reduction in PHRR, but no rating in UL-94 vertical burning test. Therefore, two challenges associated with flame-retardant coatings remain to be solved: i) poor interface adhesion to the foam substrate, and ii) low flame-retardant efficiency. In addition, the weak interface will lead to coating delamination from the PU during heating or fire, resulting in poor durability.[25] Therefore, it is of great importance to design water-based flame-retardant coatings that combine strong adhesion and outstanding flame retardancy.

Previous studies have revealed that the hydrogen (H)-bonding effect can be employed to design flame-retardant polymeric coatings with strong adhesion to the substrate.[26–29] Inspired by the H-bond adhesion mechanisms, we aim to design advanced water-based polymeric coatings by introducing flame-retardant and multi-hydroxyl groups, that combine fire-retardant and adhesive properties.[30] Herein, we have synthesized four kinds of waterborne copolymers via a facile radical copolymerization (**Figure 1**). The hydroxyl groups in 2-hydroxyethyl acrylate (HEA) and 4-hydroxybutyl acrylate (HBA) enable a strong interface adhesion to polymeric foams through interfacial H-bonding. Meanwhile, the sulfur-containing monomers serve as flame-retardant moieties, including sodium allylsulfonate (SPS), sodium vinylsulfonate (VS), and sodium p-styrenesulfonate (VSS). The sulfonate groups in these sulfur-containing monomers promote the formation of a char layer during combustion and release non-flammable gases (e.g., water vapor, sulfur dioxide) during degradation of the polymer coatings. The non-flammable gases can dilute the fuel gases and oxygen on the foam surface, thereby reducing the oxidation rate of the fuel gases and starving the flame to inhibit combustion.[31,32] The results show that among four kinds of waterborne copolymers, poly(VS-*co*-HEA) treated RPU foam exhibits the highest shear strength of 0.24 MPa, an LOI as high as 36.4 vol%, a desirable UL-94 V-0 rating, and a PHRR reduction of 34.1%. This work offers a facile biomimetic approach to synthesize water-based fire-proof polymeric coatings with strong interface adhesion to PUF, which holds promise in building insulation materials applications.

2. Experimental Section

2.1. Materials

Sodium allylsulfonate (SPS, 90% purity), sodium vinylsulfonate (VS, 25 wt%), sodium p-styrenesulfonate (VSS, >98% purity), HBA (97 wt%), and HEA (96 wt%) were purchased from Shanghai Aladdin Biochemical Technology Co., Ltd. Potassium persulfate ($K_2S_2O_8$, AR) was obtained from China National Pharmaceutical Group Chemical Reagent Co., Ltd. Dialysis bags (3500D) were acquired from Shanghai Yuan Ye Biotechnology Co., Ltd. All chemical reagents used in this chapter were utilized without further purification.

2.2. Synthesis of Sulfur-Containing Copolymers

Take the poly(SPS-*co*-HEA) as an example: the polymerization of SPS and HEA (SPS/HEA = 50:50, molar ratio) was conducted in a 500 mL four-neck round bottom flask equipped with a mechanical stirrer, a thermometer, a condenser, and N_2 inlet. First, 33.3 g of SPS was dissolved in 286.7 g of deionized water, and then the mixture was heated up to 65 °C. Subsequently, 21.7 g HEA was added dropwise to the above solution and stirred for 0.5 h until two types of monomers were mixed homogeneously. Then, 0.51 g of $K_2S_2O_8$ with 51 g of deionized water was slowly dropped into the above mixture. The polymerization continued at 65 °C for 1 h. Finally, to obtain a poly(SPS-*co*-HEA) aqueous solution with a solid concentration of 15 wt%, the dialysis and drying process were conducted to remove the residual monomer and the excess water.

Likewise, poly(SPS-*co*-HBA), poly(VS-*co*-HEA), and poly(VSS-*co*-HBA) were synthesized by the same synthesis protocol with adjusting the starting agents. After multiple dialysis steps, the solutions of poly(SPS-*co*-HEA), poly(SPS-*co*-HBA), and poly(VS-*co*-HEA) appeared colorless, while the poly(VSS-*co*-HEA) solution had a light yellow color (Figure S1, Supporting Information).

2.3. Preparation of Sulfur-Containing Polymer Films

These four polymers, poly(SPS-*co*-HEA), poly(SPS-*co*-HBA), poly(VS-*co*-HEA), and poly(VSS-*co*-HEA), were individually

L.-C. Tang
Key Laboratory of Organosilicon Chemistry and Material Technology of MoE
College of Material
Chemistry and Chemical Engineering
Hangzhou Normal University
Hangzhou 311121, China
G. Huang
School of Pharmaceutical and Chemical Engineering
Taizhou University
Taizhou 318000, China
E-mail: huangguobo@tzc.edu.cn
P. Song
School of Agriculture and Environmental Science
Centre for Future Materials
University of Southern Queensland
Springfield, QLD 4300, Australia
E-mail: pingan.song@usq.edu.au

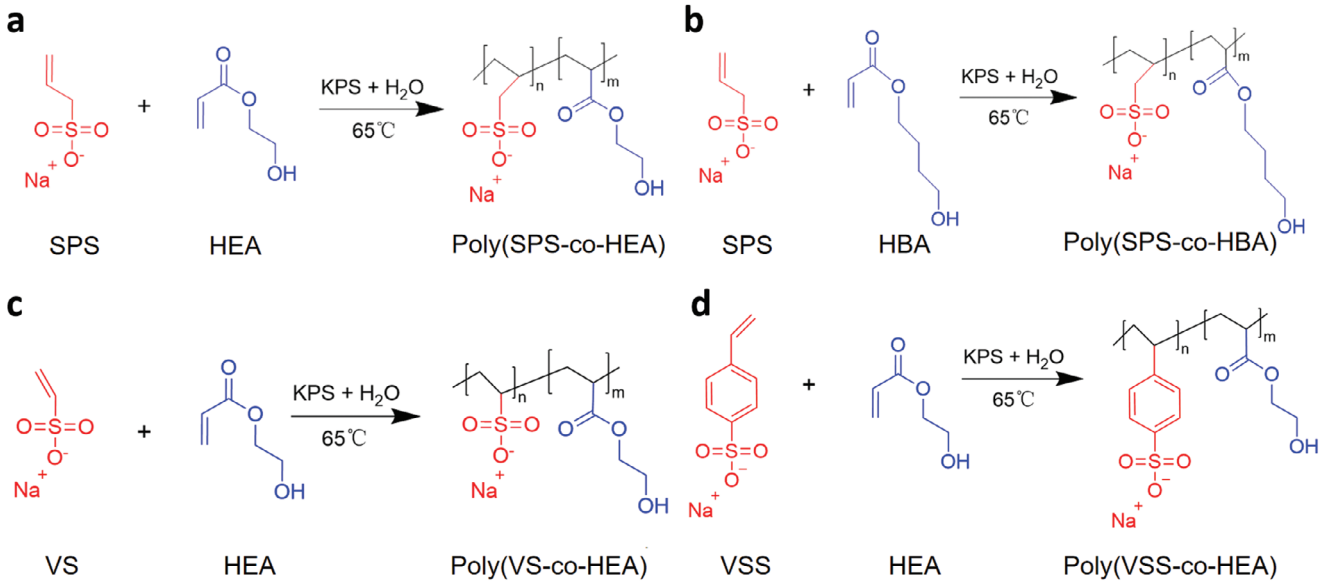

Figure 1. Synthetic route of flame retardant copolymers, a) poly(SPS-*co*-HEA), b) poly(SPS-*co*-HBA), c) poly(VS-*co*-HEA) synthesis, and d) poly(VSS-*co*-HEA).

poured into polytetrafluoroethylene (PTFE) culture dishes, followed by drying at 80 °C under a vacuum for 72 h. Finally, the sulfur-containing polymer films were obtained (Figure S2, Supporting Information). Each film was cut into the required dimensions for subsequent testing.

2.4. Fabrication of PUF Coated with Copolymers

The untreated rigid PUF was cut into the desired shapes and sizes. The copolymer aqueous solution with a concentration of 15 wt% was previously prepared. The precise thickness of the pure PUF was first measured, and the copolymer solution was uniformly applied to the PUF surface and scraped flat with a rod, followed by drying in a blast oven at 65 °C (see **Figure 2**). After complete drying, the thickness of the coated PUF was measured. Then, the copolymer solutions were repeatedly and uniformly applied onto the PUF surface. The samples were dried repeatedly until the thickness of poly(SPS-*co*-HEA), poly(SPS-*co*-HBA), poly(VS-*co*-HEA), or poly(VSS-*co*-HEA) coatings reached ≈600 µm. Finally, the coated PUF with the controlled thickness was obtained.

2.5. Characterization

FTIR spectra were recorded over the range of 4000–400 cm^{-1} on a Thermo Nicolet iS5 instrument using KBr pellets. Elemental analysis (EA) was performed on the Elementar Vario Micro instrument (Germany). Gel permeation chromatography

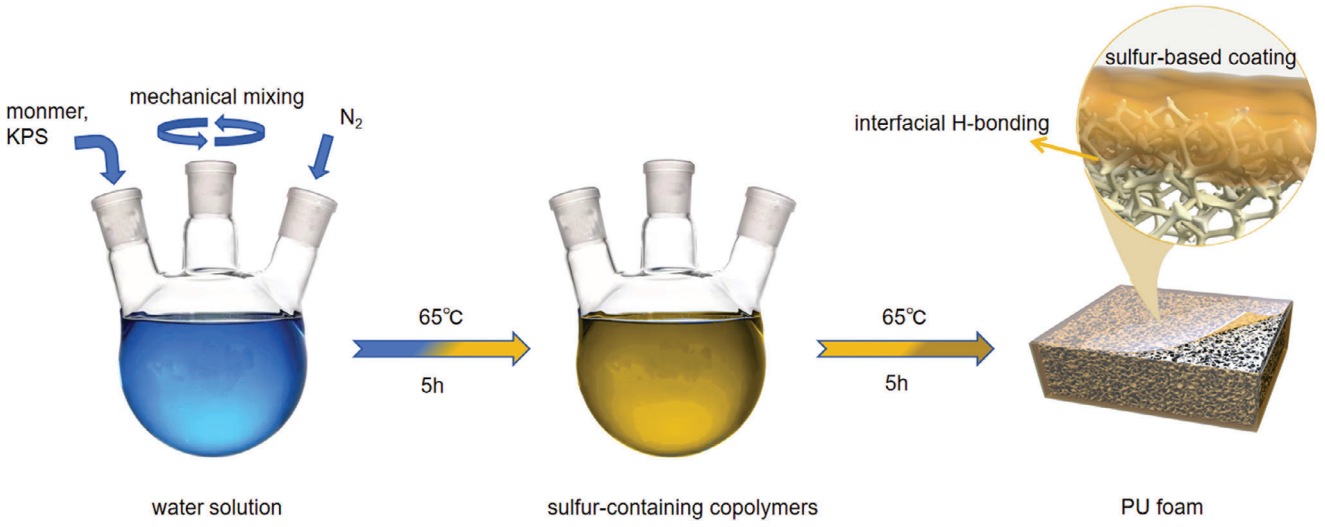

Figure 2. Schematic illustration for the preparation process of coated PUF.

(GPC) data of copolymers, including the weight-average (Mw) and number-average (Mn) molecular weights, were obtained by a gel permeation chromatograph (PL-GPC 220, Wyatt).

Differential scanning calorimetry (DSC, TA, Q20, USA) was used to record the glass transition temperature (T_g) of copolymers. Samples were heated from −50 to 65 °C at a rate of 10 °C min^{-1} and then kept isothermally for 2 min before being quenched to −50 °C, and finally reheated to 300 °C at a rate of 10 °C min^{-1}. Thermogravimetric analysis was performed on a NETZSCH TG209F3 thermal analyzer. Approximately 6 mg of copolymer samples were heated from room temperature to 800 °C under a nitrogen atmosphere with a heating rate was 20 °C min^{-1}.

Micro combustion calorimetry (MCC) was performed on a microscale combustion calorimeter (MCC-2, Govmark, USA) by heating samples from 60 to 700 °C at a heating rate of 1 K s^{-1} under an air atmosphere. Vertical burning (UL-94) test was performed via a CFZ-3 instrument based on ASTM D 3801–96 standard. The LOI was measured on a JF-3 oxygen index instrument based on ASTM D 2863–97 standard. A cone calorimeter test (CCT) was conducted to investigate the combustion behavior of materials by using an FTT cone calorimeter at the heat flux of 35 kW m^{-2} according to the standard ISO 5660.

A universal testing machine was employed to measure the shear tensile adhesion stress based on the ASTM F2255 standard. Interface adhesion test was conducted according to GB/T 33334-2016. A microscopic Vickers hardness tester (MHVS-1000T) was conducted to measure the hardness of these polymeric coatings. UV aging test was conducted by using a UVA-365 LED UV curing lamp. The polymeric films were exposed to UV lamps with a power of 20 W and UV wavelength of 365 nm for a cumulative period of 72 h, and the surface of the samples was observed under an optical microscope at 0, 24, 48, and 72 h. The friction wear test was conducted by using a UMT-2 friction wear tester, and the normal load was 1 N. Tensile testing was conducted using an electronic universal testing machine, Meters Industrial Systems (China) Limited, Model CMT6104, in accordance with ASTM D882 standard. Three sets of polymer film tensile properties were measured at 22 °C and 55% relative humidity.

3. Results and Discussion

3.1. Characterization of Copolymers

The FTIR spectra of four polymer groups are depicted in Figure S3, Supporting Information. For poly(SPS-*co*-HEA), the absorption peak at 3391 cm^{-1} corresponds to the stretching vibration of alcohol hydroxyl groups (O—H). The peak at 3000–2800 cm^{-1} represents the stretching vibration of saturated C—H bonds. The absorption peak at 1717 cm^{-1} is associated with the stretching vibration of ester carbonyl groups (C═O).[33] Other notable peaks include 1449 cm^{-1} for methylene variable-angle vibration and asymmetric methyl variable-angle vibration, 1395 cm^{-1} for symmetric methyl variable-angle vibration, and 1159 and 1073 cm^{-1} for asymmetric and symmetric stretching vibrations of sulfonic acid salts.[34] Additionally, there are peaks at 1036 cm^{-1} for stretching vibrations of alcohol and ester C—O, and 892 cm^{-1} for stretching vibrations of S—O.[35]

Table 1. M_n, M_w, M_z, M_{z+1}, and PDI of different copolymers.

Samples	M_n [g mol^{-1}]	M_w [g mol^{-1}]	M_z [g mol^{-1}]	M_{z+1} [g mol^{-1}]	PDI[a)]
Poly(SPS-*co*-HEA)	5199	14 095	30 381	50 071	2.71
Poly(SPS-*co*-HBA)	1623	2992	4723	6230	1.84
Poly(VS-*co*-HEA)	8810	31 747	61 136	85 163	3.60
Poly(VSS-*co*-HEA)	41 385	73 478	103 605	124 782	1.78

[a)] PDI refers to polydispersity index.

Similar to poly(SPS-*co*-HEA), poly(SPS-*co*-HBA) and poly(VSS-*co*-HEA) exhibit the characteristic peaks of saturated C—H stretching vibrations, ester carbonyl stretching vibrations, and various methyl variable-angle vibrations. Notably, for poly(SPS-*co*-HBA), there is an additional peak at 2960 cm^{-1} associated with the out-of-plane bending vibration of trans-double-substituted —CH—.[36] While for poly(VSS-*co*-HEA), there are some characteristic peaks at 1078, 1036, and 1009 cm^{-1} corresponding to the in-plane bending vibrations of the benzene ring, and the peak at 794 cm^{-1} for the out-of-plane bending vibration of the benzene ring.[37] The strong peak at 567 cm^{-1} is attributed to the stretching vibration of C—S.[38] EA results show that the H, C, O, and S elements proportions in poly(SPS-*co*-HEA), poly(SPS-*co*-HBA), poly(VS-*co*-HEA), and poly(VSS-*co*-HEA) are relatively similar (Table S1, Supporting Information).

GPC data shows that the molecular weight follows the sequence of poly(SPS-*co*-HBA) < poly(SPS-*co*-HEA) < poly(VS-*co*-HEA) < poly(VSS-*co*-HEA) (**Table 1**). In particular, the molecular weight of poly(VSS-*co*-HEA) is significantly higher than the other three polymers, indicating that poly(VSS-*co*-HEA) has longer polymer chains and a higher degree of polymerization. Additionally, poly(VSS-*co*-HEA) has the lowest polydispersity index (PDI), suggesting that the distribution of molecular weights within poly(VSS-*co*-HEA) is more uniform and less varied. In other words, the poly(VSS-*co*-HEA) chains have similar or closer molecular weights, contributing to a more homogeneous composition. This is often desirable in polymer chemistry as it suggests a more consistent and controlled synthesis of the polymer.

3.2. Thermal, Flame-Retardant, Mechanical, and Adhesive Properties

The excellent compatibility of copolymers as a potential surface coating on PUF surfaces in various temperature environments is crucial. As shown in **Figure 3**, the presence of more flexible poly-HBA segments imparts poly(SPS-*co*-HBA) with lower glass transition temperatures (T_g) compared to poly(SPS-*co*-HEA) and/or poly(VS-*co*-HEA). Furthermore, all the polymers exhibit multiple T_g values, for example, −36 and −8 °C in poly(VSS-*co*-HBA) correspond to the glass transition behavior of two homopolymer chain segments, respectively, whereas the low T_g value of the polyHEA segments ensures the flexibility of the coating in low-temperature environments, which is essential for their use.[39]

Prior to practical application, flame-retardant coatings are required to exhibit excellent flame retardancy, good thermal stability, and char formation properties. MCC curves and the related

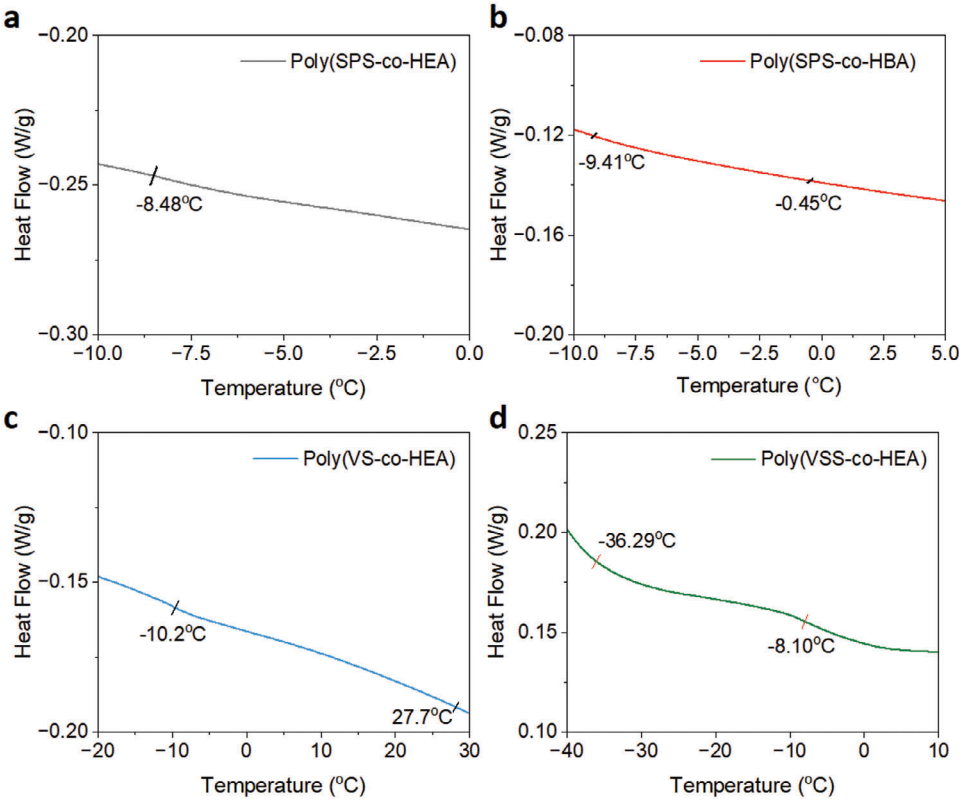

Figure 3. DSC curves of flame retardant copolymers, a) poly(SPS-*co*-HEA), b) poly(SPS-*co*-HBA), c) poly(VS-*co*-HEA) synthesis, d) poly(VSS-*co*-HEA).

data of four copolymer films are depicted in **Figure 4** and Table S2, Supporting Information. All copolymers demonstrate inherent flame retardancy, as evidenced by the poly(VS-*co*-HEA) with a PHRR as low as 42.8 W g^{-1} at 395 s and a total heat release (THR) of only 3.34 kJ g^{-1}, which provides the best HRR suppression among the four copolymers. This is due to the presence of fewer methylene groups with higher calorific values in its chain structure.[40] On the contrary, the most intense heat release occurs in poly(SPS-*co*-HBA), with a PHRR value as high as 87.6 W g^{-1} and THR of 9.07 kJ g^{-1}, along with two intense heat release peaks at 305 and 390 s, respectively. On the other hand, the low heat release of poly(VSS-*co*-HEA) can be attributed to its abundant sp^2 carbon, which facilitates the formation of stable graphitic structures at high temperatures.[41,42] It can be observed that poly(VS-*co*-HEA) has the lowest PHRR among the four tested groups. This indicates that PUF coated with flame-retardant polymers releases heat at a slower rate under combustion conditions. The small heat load during a fire is crucial for reducing the damage of the fire to the surrounding environment and structures.

TGA curves and the related data of the four flame-retardant copolymer coatings are depicted in **Figure 5** and **Table 2**. Likewise, poly(VSS-*co*-HEA) copolymer shows the best charring

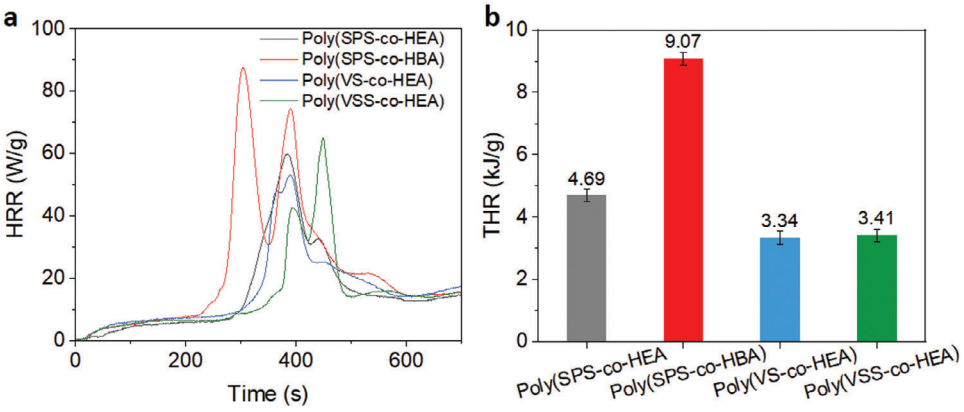

Figure 4. HRR curves and THR values of flame retardant copolymers.

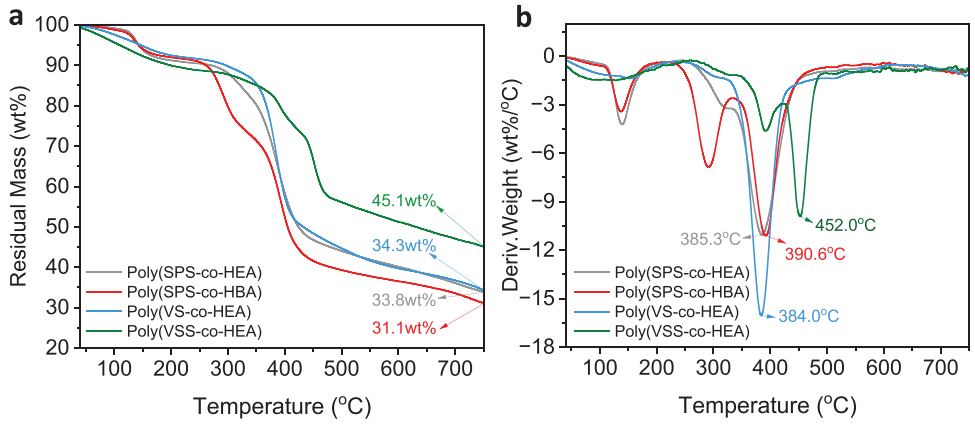

Figure 5. TGA and DTG curves of four kinds of fire-retardant copolymers.

capacity with significantly higher residual char of 43.3 wt%, which is predominantly stabilized inorganic sodium salts (from the sodium sulphonate groups) and graphitized char layers (from the phenyl side chains).[43,44] Additionally, poly(VSS-*co*-HEA) and poly(VS-*co*-HEA) have a much slower decomposition process, which is also demonstrated by avoiding the drastic thermal weight loss at 125 and 275 °C. In contrast, poly(SPS-*co*-HBA) with higher carbon and hydrogen content only exhibits a char residue as low as 31.1 wt%, and multiple distinct degradation processes are observed as the temperature increases (at 140, 290, and 390 °C).

In this work, PUF is selected as a representative substrate to verify the fire protection of copolymers. Therefore, it is necessary to ensure the required mechanical properties of the coatings and their adhesion to the PUF before practical application. The films of poly(SPS-*co*-HEA) and poly(VS-*co*-HEA), respectively, show a tensile strength of 1.42 and 0.85 MPa, higher than poly(SPS-*co*-HBA) (0.48 MPa) (see Figure S4, Supporting Information). As shown in **Figure 6**, the evaluation of the interfacial adhesion of several copolymers to the PUF matrix based on shear strength follows the order: poly(VS-*co*-HEA) (0.24 MPa) > poly(SPS-*co*-HEA) (0.23 MPa) > poly(SPS-*co*-HBA) (0.18 MPa) > poly(VSS-*co*-HEA) (0.14 MPa). The highest adhesion of poly(VS-*co*-HEA) is largely attributed to the high polarity of polyHEA and its abundant hydroxyl groups to form strong interfacial H-bonding.[45] As a result, the PUF substrate is the first to fracture during single-targeted stretching, implying that the bond strength exceeds the fracture strength. In contrast, the weakest adhesion of poly(VSS-*co*-HEA) leads to the detachment of the coating from the PUF surface during the curing stage, preventing subsequent performance testing (Figure S5, Supporting Information).

To visually evaluate the fire protection of copolymer coatings on PUF surfaces, UL-94 vertical burning and LOI tests are conducted, and the related data are shown in **Table 3**. Due to its inherent flammability and porous structure, PUF achieves no ratings in the UL-94 test and exhibits an LOI value as low as 19.1 vol%. During the UL-94 test, PUF is immediately ignited with a rapid flame spread to the fixture until burned out, leaving a very fragile and hollow char after testing (Figure S6, Supporting Information). Upon treatment with poly(VS-*co*-HEA) or other copolymer coatings (see Figure S7, Supporting Information), satisfactory LOI values of 36.4% are achieved for the treated foam, meeting the required UL-94 V-0 rating. It is noteworthy that when SPS is employed as a flame-retardant monomer, the presence of more high calorific value methylene favors flame maintenance, which may be responsible for its decreased LOI values, for example, 32.4% and 31.5% for poly(SPS-*co*-HEA)-PUF and poly(SPS-*co*-HBA)-PUF, respectively (Table 3).[46]

Further evaluation of the coated PUF in real fire scenarios and cone calorimetry tests were conducted. The thickness of the coat-

Table 2. TGA data for fire-retardant copolymers.

Samples	T_i [a)] [°C]	T_{max} [a)] [°C]	$Char_{750\,°C}$ [wt%]
Poly(SPS-*co*-HEA)	143	385.3	33.8
Poly(SPS-*co*-HBA)	142	390.6	31.1
Poly(VS-*co*-HEA)	147	384	34.3
Poly(VSS-*co*-HEA)	109	452	45.1

[a)] T_i and T_{max} refer to the temperature at 5% weight loss and the temperature at the maximum weight loss rate.

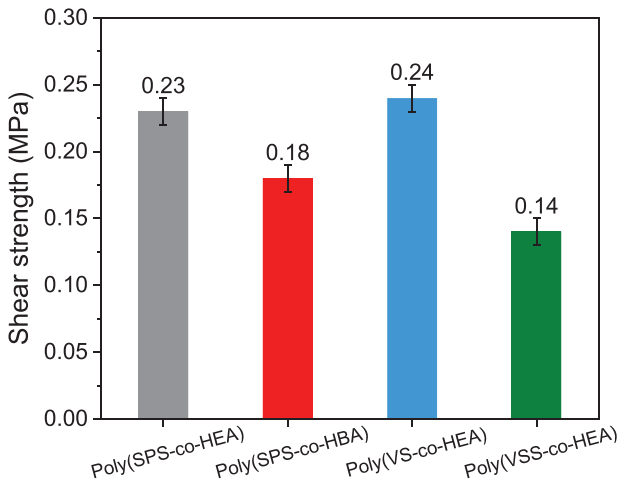

Figure 6. Shear stress values of flame-retardant coatings on PUF.

Table 3. Detailed CCT, UL-94, and LOI data for PUF and the coated PUF foams.

Samples	t_{ign}[a] [s]	PHRR[a] [kW m^{-2}]	t_{PHRR}[a] [s]	THR[a] [MJ m^{-2}]	TSR[a] [m^2 m^{-2}]	ACOY[a] [kg kg^{-1}]	PSPR[a] [m^2 s^{-1}]	UL-94 rating	LOI [vol%]
PUF	4 ± 1	252 ± 5	60 ± 2	99 ± 2	1102 ± 5	0.05 ± 0.01	0.076±0.005	No rating	19.1
Poly(SPS-*co*-HEA)-PUF	30 ± 1	145 ± 5	165 ± 2	158 ± 2	1089 ± 5	0.10 ± 0.01	0.016±0.005	V-0	32.4
Poly(SPS-*co*-HBA)-PUF	38 ± 1	195 ± 5	67 ± 2	148 ± 2	905 ± 5	0.04 ± 0.01	0.026±0.005	V-0	31.5
Poly(VS-*co*-HEA)-PUF	35 ± 1	166 ± 5	103 ± 2	144 ± 2	1403 ± 5	0.02 ± 0.01	0.022±0.005	V-0	36.4

[a] t_{ign}, PHRR, t_{PHRR}, THR, TSR, ACOY, and PSPR are the time to ignition, peak heat release rate, time to peak heat release rate, total heat release, total smoke release, average carbon monoxide yield, and peak smoke production rate, respectively.

ing in the CCT test was consistent with those of the other coatings tested, which were 600 µm. Cone calorimetry tests provide some crucial fire parameters such as time to ignition (t_{ign}), HRR, THR, mass loss, smoke production rate (SPR), and average CO yield (ACOY). At an external heat flow radiation, the PUF exhibits an extremely short ignition process, ≈4 s, and reaches a PHRR of 252 kW m^{-2} at 60 s, corresponding to the sharp thermal decomposition of the foam, ultimately resulting in a THR of 99 MJ m^{-2} (**Figure** 7a,b). In contrast, the t_{ign} of the coated PUF is significantly prolonged, ranging from 30 to 38 s, with varying degrees of PHRR reduction, corresponding to the formation of more stable organic and/or inorganic char layers on the top surface during the combustion process.[47] On the other hand, the increase in THR is attributed to the intrinsic heat release of the organic coating, leading to prolonged smoldering accompanied by gradual heat accumulation.[48] The sulfonate groups on the branched chains are the source of flame retardancy for all coatings, and therefore the differences in the heat release parameters of the foam materials treated with these coatings are not significant.[49] Interestingly, poly(SPS-*co*-HEA)-PUF and poly(VS-*co*-HEA)-PUF exhibit lower PHRR and longer t_{PHRR}, reaching 145 kW m^{-2} at 165 s and 166 kW m^{-2} at 103 s, respectively, which is also attributed to the lower heat release contribution of polyHEA compared to polyHBA (Table 3).

The fire performance index (FPI) and fire growth index (FGI), two key parameters for evaluating the fire performance of materials, are calculated. Generally, higher FPI and lower FGI values reflect superior fire safety.[50] Therefore, the low FPI value of 0.016 m^2 s kW^{-1} and the FGI value of 4.191 kW m^{-2} s^{-1} for PUF indicate its high flammability and significant fire hazard (Figure 7c,d). In contrast, all coatings increase the FPI values of the foam to varying degrees and decrease their FGI, with the advantage being particularly pronounced when using polyHEA as a film-forming component. For example, poly(VS-*co*-HEA) coating

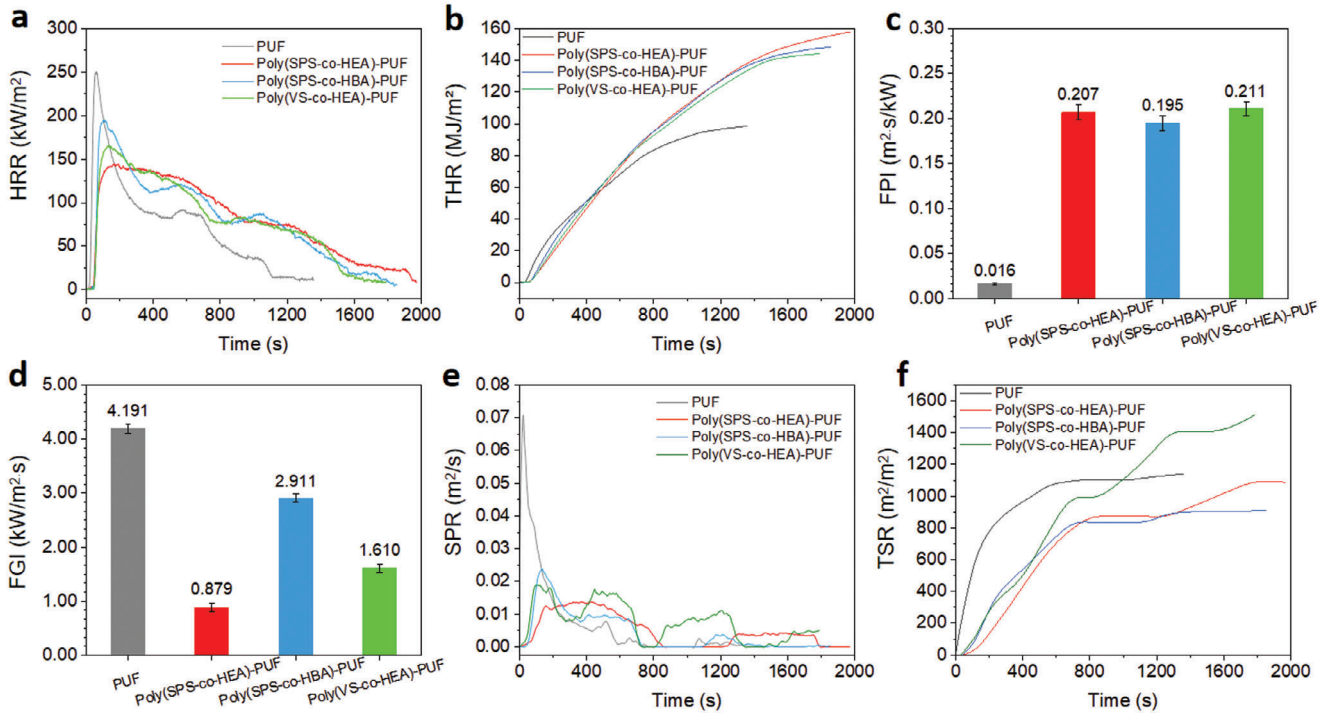

Figure 7. a) HRR, b) THR, c) FPI, d) FGI, e) SPR, and f) TSR curves of coated PUFs.

results in a PUF with an FPI of 0.211 m^2 s kW^{-1} and an FGI of 1.610 kW m^{-2} s^{-1}, ≈13 folds and 38% of those of the neat PUF, respectively, further demonstrating its reduced fire hazard, demonstrating its reduced fire risk (Figure 7c,d).

Smoke/gas release is another important indicator in assessing the fire safety of polymeric materials. Specifically, all copolymer coatings can significantly reduce the peak smoke production rate (PSPR) and ACOY of PUFs. For instance, poly(VS-*co*-HEA)-PUF has a PSPR of 0.022 m^2 s^{-1} and an ACOP of 0.02 kg kg^{-1}, which are 71% and 62% lower than those of PUF, respectively (Figure 7e and Table 3). This appreciable reduction is primarily attributed to the formation of an integral sulfonated carbon (Figure S8, Supporting Information). A protective char residue whose high thermal stability has been previously demonstrated,[51] acts as a barrier hindering mass transfer and effectively reduces the thermal decomposition rate of the underlying substrate.[52] Furthermore, among the three groups of coated PUF, poly(SPS-*co*-HBA)-PUF had the highest PSPR of 0.026 m^2 s^{-1}, once again highlighting that excessive methylene structure in the branched chain can exacerbate the early smoke release of the coating (Figure 7e). While the presence of organic coatings can mitigate the early-stage smoldering of the substrate, it ultimately cannot prevent decomposition during prolonged burning, resulting in the TSR values of the coated PUF remaining within the same order of magnitude as the neat PUF (Figure 7f).[53]

The weathering resistance of the three flame-retardant coatings was further characterized for the practical application scenarios of as-prepared coatings. After 72 h of UV exposure, no significant morphology change was observed on poly(VS-*co*-HEA), indicating its desired UV aging resistance (see Figure S9, Supporting Information). In addition, the low coefficient of friction (as low as 0.115) and high hardness indicate its robust durability (see Figures S10 and S11, Supporting Information). These properties highlight the potential of poly(VS-*co*-HEA) as a high-performance coating material for a wide range of applications that require long-term stability and wear resistance.

4. Conclusions

In this work, four sulfur-containing flame-retardant copolymers poly(SPS-*co*-HEA), poly(SPS-*co*-HBA), poly(VS-*co*-HEA), and poly(VSS-*co*-HEA) have been synthesized via a facile radical copolymerization. All these copolymeric coatings demonstrate good charring ability and inherent flame retardancy with low PHRR values of <90 W g^{-1}. Although the thermal stability of poly(VSS-*co*-HEA) is the best among the four copolymers, the interface adhesion with PUF is not suitable for PUF coating as a result of its strong polarity. Poly(SPS-*co*-HEA), poly(SPS-*co*-HBA), and poly(VS-*co*-HEA) are employed to treat PUF as fire-retardant coatings. The presence of 600 µm their coatings enables PUF to achieve a UL-94 V-0 rating. With poly(VS-*co*-HEA) coating, the treated PUF foam exhibits the highest LOI value of 36.4 vol% and a PHRR reduction of 34.1%, indicating its highest fire-retardant efficiency. Meanwhile, it exhibits the strongest interface adhesion to PUF with a shear strength of 0.24 MPa. This work offers a facile and efficient approach to preparing high-performance water-borne coatings for PUF which could be expected to demonstrate potential applications as building insulation materials.

Supporting Information

Supporting Information is available from the Wiley Online Library or from the author.

Acknowledgements

Thanks are given to Miss Pan Yang for her help in drying samples. This work was financially supported by the Plan of Youth Innovation Team for Universities of Shandong Province (Grant No. 2023KJ099), and the Australian Research Council (Grant No. FT190100188, LP220100278, DP240102628, DP240102728).

Open access publishing facilitated by University of Southern Queensland, as part of the Wiley - University of Southern Queensland agreement via the Council of Australian University Librarians.

Conflict of Interest

The authors declare no conflict of interest.

Data Availability Statement

The data that support the findings of this study are available in the supplementary material of this article.

Keywords

fire retardant, fire-retardant coatings, polyurethane foam, sulfur-containing polymers

Received: January 31, 2024
Revised: March 31, 2024
Published online: April 9, 2024

[1] M. Zhu, Z. Ma, L. Liu, J. Zhang, S. Huo, P. Song, *J. Mater. Sci. Technol.* **2022**, *112*, 315.
[2] A. Yadav, F. M. de Souza, T. Dawsey, R. K. Gupta, *Ind. Eng. Chem. Res.* **2022**, *61*, 15046.
[3] X.-L. Chen, F.-R. Zeng, W.-X. Li, L. Zhang, C. Deng, Y. Tan, M.-J. Chen, S.-C. Huang, B.-W. Liu, Y.-Z. Wang, *J. Mater. Sci. Technol.* **2023**, *162*, 179.
[4] Z.-J. Cao, X. Dong, T. Fu, S.-B. Deng, W. Liao, Y.-Z. Wang, *Polym. Degrad. Stab.* **2017**, *136*, 103.
[5] B. Gouteux, M. Alaee, S. A. Mabury, G. Pacepavicius, D. C. Muir, *Environ. Sci. Technol.* **2008**, *24*, 9039.
[6] K.-Y. Guo, Q. Wu, M. Mao, H. Chen, G.-D. Zhang, L. Zhao, J.-F. Gao, P. Song, L.-C. Tang, *Composites, Part B* **2020**, *193*, 108017.
[7] O. D. Ekpe, G. Choo, D. Barceló, J. E. Oh, *Compr. Anal. Chem.* **2020**, *88*, 1.
[8] H. Yang, L. Song, Y. Hu, R. K. Yuen, *Polym. Adv. Technol.* **2018**, *29*, 2917.
[9] Y. Yuan, W. Wang, Y. Shi, L. Song, C. Ma, Y. Hu, *J. Hazard.* **2020**, *382*, 121028.
[10] Z.-J. Cao, W. Liao, S.-X. Wang, H.-B. Zhao, Y.-Z. Wang, *Chem. Eng. J.* **2019**, *361*, 1245.
[11] W. Dukarski, I. Rykowska, P. Krzyżanowski, M. Gonsior, *Fire* **2024**, *7*, 50.
[12] M. Liu, B. Peng, G. Su, M. Fang, *Environ. Sci. Technol.* **2021**, *55*, 14477.
[13] M. Grdadolnik, B. Zdovc, A. Drinčić, O. C. Onder, P. Utroša, S. G. Ramos, E. D. Ramos, D. Pahovnik, E. Zagar, *ACS Sustainable Chem. Eng.* **2023**, *11*, 10864.

[14] L. Liu, Y. Xu, M. Xu, Y. He, S. Li, B. Li, *Mater. Des.* **2020**, *187*, 108302.
[15] F. Teles, G. Martins, F. Antunes, *J. Anal. Appl. Pyrolysis* **2022**, *163*, 105466.
[16] Y. Yuan, H. Yang, B. Yu, Y. Shi, W. Wang, L. Song, Y. Hu, Y. Zhang, *Ind. Eng. Chem. Res.* **2016**, *55*, 10813.
[17] L. Liu, J. Feng, Y. Xue, V. Chevali, Y. Zhang, Y. Shi, L. C. Tang, P. Song, *Adv. Funct. Mater.* **2023**, *33*, 2212124.
[18] H. Yang, X. Wang, L. Song, B. Yu, Y. Yuan, Y. Hu, R. K. Yuen, *Polym. Adv. Technol.* **2014**, *25*, 1034.
[19] Y. Yuan, C. Ma, Y. Shi, L. Song, Y. Hu, W. Hu, *Mater. Chem. Phys.* **2018**, *211*, 42.
[20] L. Liu, M. Zhu, J. Feng, H. Peng, Y. Shi, J. Gao, L. C. Tang, P. Song, *Aggregate.* **2024**, https://doi.org/10.1002/agt2.494.
[21] Z. Ma, J. Zhang, L. Liu, H. Zheng, J. Dai, L.-C. Tang, P. Song, *Compos. Commun.* **2022**, *29*, 101046.
[22] Y. Xue, T. Zhang, H. Peng, Z. Ma, M. Zhang, M. Lynch, T. Dinh, Z. Zhou, Y. Zhou, P. Song, *Nano Res.* **2024**, *17*, 2186.
[23] H. B. Chen, P. Shen, M. J. Chen, H. B. Zhao, D. A. Schiraldi, *ACS Appl. Mater. Interfaces* **2016**, *8*, 32557.
[24] Y. Huang, S. Jiang, R. Liang, P. Sun, Y. Hai, L. Zhang, *Chem. Eng. J.* **2020**, *391*, 123621.
[25] H. Somarathna, S. Raman, D. Mohotti, A. Mutalib, K. Badri, *Constr. Build. Mater.* **2018**, *190*, 995.
[26] Z. Ma, X. Liu, X. Xu, L. Liu, B. Yu, C. Maluk, G. Huang, H. Wang, P. Song, *ACS Nano* **2021**, *15*, 11667.
[27] X. Li, Z. Zhao, Y. Wang, H. Yan, X. Zhang, B. Xu, *Chem. Eng. J.* **2017**, *324*, 237.
[28] L. Liu, M. Zhu, X. Xu, X. Li, Z. Ma, Z. Jiang, A. Pich, H. Wang, P. Song, *Adv. Mater.* **2021**, *33*, 2105829.
[29] L. Liu, M. Zhu, Z. Ma, X. Xu, J. Dai, Y. Yu, S. M. Seraji, H. Wang, P. Song, *Chem. Eng. J.* **2022**, *440*, 135645.
[30] F. F. Li, *Molecules* **2023**, *28*, 1842.
[31] S. V. Levchik, E. D. Weil, *J. Fire Sci.* **2006**, *24*, 345.
[32] X. Sheng, X. Jiang, H. Zhao, D. Wan, Y. Liu, C. A. Ngwenya, L. Du, *Spectrochim. Acta, Part A* **2018**, *198*, 239.
[33] G. Laufer, C. Kirkland, A. B. Morgan, J. C. Grunlan, *ACS Macro Lett.* **2013**, *2*, 361.
[34] B. I. Dogaru, V. Stoleru, G. Mihalache, S. Yonsel, M. C. Popescu, *Molecules* **2021**, *26*, 5755.
[35] L. Larsen, C. Nielsen, *J. Chem. Soc. Faraday Trans.* **1998**, *94*, 2277.
[36] N. Pasadakis, G. Livanos, M. Zervakis, *Spectroscopy* **2013**, *10*, 25.
[37] V. Udayakumar, S. Periandy, M. Karabacak, S. Ramalingam, *Spectrochim. Acta, Part A* **2011**, *83*, 575.
[38] P. Siriphannon, Y. Kameshima, A. Yasumori, K. Okada, S. Hayashi, *J. Eur. Ceram. Soc.* **2002**, *22*, 511.
[39] J. Kwon, H. Cho, H. Eom, H. Lee, Y. D. Suh, H. Moon, J. Shin, S. Hong, S. H. Ko, *ACS Appl. Mater. Interfaces* **2016**, *8*, 11575.
[40] S. J. Lee, M. Y. Choi, A. R. Lim, *ACS Omega* **2021**, *6*, 15392.
[41] D. Kong, Z. Xiao, Y. Gao, X. Zhang, R. Guo, X. Huang, X. Li, L. Zhi, *Mater. Sci. Eng.: R: Rep.* **2019**, *137*, 1.
[42] W. Qu, X. Han, J. Liu, L. Yin, C. Liang, P. Hu, *Green Chem.* **2023**, *25*, 9873.
[43] J. Munuera, J. Paredes, S. Villar-Rodil, M. Ayán-Varela, A. Martínez-Alonso, J. Tascón, *Nanoscale* **2016**, *8*, 2982.
[44] H. W. Shim, K. J. Ahn, K. Im, S. Noh, M. S. Kim, Y. Lee, H. Choi, H. Yoon, *Macromolecules* **2015**, *48*, 6628.
[45] L. Chen, J. Xu, M. Zhu, Z. Zeng, Y. Song, Y. Zhang, X. Zhang, Y. Deng, R. Xiong, C. Huang, *Mater. Horiz.* **2023**, *10*, 4000.
[46] R. Singh, B. Ruj, A. Sadhukhan, P. Gupta, V. Tigga, *Fuel* **2020**, *262*, 116539.
[47] B. W. Liu, H. B. Zhao, Y. Z. Wang, *Adv. Mater.* **2022**, *34*, 2107905.
[48] H. Feng, D. Li, B. Cheng, T. Song, R. Yang, *J. Hazard. Mater.* **2022**, *424*, 127420.
[49] T. Sai, S. Ran, S. Huo, Z. Guo, P. Song, Z. Fang, *Chem. Eng. J.* **2022**, *433*, 133264.
[50] X. Zhou, S. Qiu, L. He, X. Wang, Y. Zhu, F. Chu, B. Wang, L. Song, Y. Hu, *Chem. Eng. J.* **2021**, *425*, 130655.
[51] J. M. Fonseca, L. Spessato, A. L. Cazetta, C. da Silva, V. D. C. Almeida, *Chem. Eng. Process.* **2022**, *170*, 108668.
[52] F. Herold, J. Gläsel, B. J. Etzold, M. Rønning, *Chem. Mater.* **2022**, *34*, 8490.
[53] O. Y. Wen, M. Z. M. Tohir, T. C. S. Yeaw, M. A. Razak, H. S. Zainuddin, M. R. A. Hamid, *Prog. Org. Coat.* **2023**, *175*, 107330.

